Supporting Information

Lai et al. 10.1073/pnas.1211431109

SI Methods

Animals. Dystrophin-deficient mdx mice were purchased from The Jackson Laboratory. Utrophin heterozygous mdx mice (*mdx/utro*$^{+/-}$) were originally provided by Mark Grady (Washington University, St. Louis, MO) (1). Experimental utrophin/dystrophin double knockout (u-dko) mice were generated by crossing *mdx/utro*$^{+/-}$ mice, as previously described (2). The skeletal muscle specific mini- and microdystrophin transgenic mdx mice were published previously (3, 4). In these transgenic mice, the mini- or microdystrophin genes were expressed under the transcriptional regulation of the human skeletal α-actin promoter. Three transgenic strains were used in the study. The ΔH2-R19 minidystrophin transgenic mdx mice were used to determine in vivo neuronal NOS (nNOS) binding by the stripped-down R16/17 construct (Fig. 1). This minigene carries the C-terminal domain but does not contain dystrophin R16/17. The ΔR4-23/ΔC and the ΔR2-R15/ΔR18-R23/ΔC microgene transgenic mdx mice were used as negative and positive controls, respectively, for nNOS binding in muscle (Fig. S3*B*). Dystrophin R16/17 is present in the ΔR2-R15/ΔR18-R23/ΔC microgene but not in the ΔR4-23/ΔC microgene. Experimental mice were housed in a specific pathogen-free animal facility.

Microdystrophins and Microutrophins. A total of 48 different microdystrophin and microutrophin constructs were used for in vivo nNOS binding assay (Table S1). A total of five different microdystrophin constructs were evaluated in vitro for their nNOS binding activity by yeast two-hybrid assay. These microgenes were generated using PCR-based cloning method and all were confirmed by DNA sequencing (Table S1). Microgene expression was regulated by the CMV promoter and SV40 polyadenylation signal. For microdystrophin cloning, a previously published human ΔR2-R15/ΔR18-R23/ΔC microgene was used as the backbone (3). All dystrophin-related modifications were made according to the human dystrophin sequence. The microutrophin genes were cloned using the full-length mouse utrophin cDNA as the template (a gift of James Ervasti, University of Minnesota, Minneapolis, MN) (5). All utrophin-related modifications were made according to the mouse utrophin sequence.

Recombinant Adeno-Associated Virus Vector and in Vivo Gene Transfer. The microgene expression cassette was cloned between two inverted terminal repeats in a *cis* AAV packaging plasmid (6). All experimental adeno-associated virus (AAV) vectors were pseudotyped using the Y445F AAV-6 tyrosine mutant capsid (a gift of Arun Srivastava, University of Florida, Gainesville, FL) (7, 8). AAV vectors were purified through two rounds of CsCl gradient ultracentrifugation and the viral titer was determined by quantitative PCR according to our published protocol (6). To test in vivo nNOS binding activity, 1×10^{10} vector genome (vg) particles of AAV vectors were directly injected into the tibialis anterior (TA) muscle of 2- to 6-mo-old mdx or transgenic mdx mice, or 3-wk-old u-dko mice (9).

Immunofluorescence Staining and nNOS Activity Staining. Freshly collected muscle samples were embedded in Tissue-Tek OCT (Sakura Finetek) and snap-frozen in 2-methylbutane with liquid nitrogen. GFP was visualized under the FITC channel using a Nikon E800 fluorescence microscope. Human dystrophin derived microdystrophin was detected with Dys-3, a human dystrophin-specific monoclonal antibody (1:20; Novocastra). This antibody recognizes an epitope in human dystrophin hinge 1. Dystrophin spectrin-like repeats 16 and 17 were detected with Mandys 102 (1:20) and Manex 44A (1:300) monoclonal antibodies, respectively (gifts from Glenn Morris, The Robert Jones and Agnes Hunt Orthopedic Hospital, Oswestry, Shropshire, United Kingdom) (3, 10). Utrophin was revealed with a mouse monoclonal antibody against the utrophin N-terminal domain (1:20; Vector Laboratories). nNOS was detected with a rabbit polyclonal antibody against an epitope near the C-terminal end of nNOS (1:2,000; Santa Cruz). Histochemical evaluation of nNOS activity was performed according to our published protocol (3, 4, 11, 12). This staining revealed the NADPH diaphorase activity of nNOS. The Flag tag was revealed with the monoclonal anti-FLAG M2 antibody (1:1,00; Sigma). Photomicrographs were taken with a Qimage Retiga 1300 camera using a Nikon E800 fluorescence microscope.

Western Blot. Whole-muscle lysate and membrane-enriched microsomal preparations were obtained from snap-frozen TA muscles according to our previously published protocols (3, 4, 11–13). ΔH2-R19 minidystrophin was detected with an antibody against the C-terminal domain of dystrophin (Dys-2, 1:100; Novocastra). Microdystrophins (including ΔR4-R23/ΔC, ΔR2-R15/ΔR18-R23/ΔC, μ-Dys+Utro R15 and μ-Dys+Utro R16) were probed with the Dys-B antibody that reacts with dystrophin R1 (1:100; Novocastra, Leica Microsystems). Mandys 102 (1:20) and Manex 44A (1:500) monoclonal antibodies were used to detect dystrophin R16 and R17, respectively. nNOS was detected with a rabbit polyclonal antibody against the N-terminal end of nNOS (1:4,000; Upstate, Millipore). α-Tubulin (1:3,000; Sigma) was used as the loading control for whole-muscle lysate Western blot. α1-Na^+/K^+ ATPase (1:400; Upstate, Millipore) was used as the loading control for microsomal preparation Western blot.

Yeast Two-Hybrid. Yeast two-hybrid assay was performed with the Matchmaker GAL4 Two-Hybrid System 3 (Clontech) as described previously (3). The nNOS PDZ domain [a gift of David Bredt (University of California, San Francisco, CA) and Samie R. Jaffrey (Cornell University Weill Medical College, New York, NY)] was cloned into the binding construct (3, 14). The activation constructs contain the α-helix–modified dystrophin R16/17 in which individual helix within R16/17 was replaced by the corresponding helix from dystrophin R18. A total of five different activation constructs were generated. In each construct, one of the following dystrophin helices including R16α1, R16α2, R16α3, R17α1, or R17α2 was replaced. All constructs were sequenced before use. The positive control for the yeast two-hybrid assay was performed using the syntrophin PDZ domain as the activation construct according to our previous publication (3). To detect positive interaction, the binding construct and one of the referred activation construct were cotransfected to yeast cells. The qualitative plate assay and the semiquantitative dot assay were performed on the leucine/tryptophan/histidine triple-deficient medium. The quantitative β-galactosidase activity assay was measured using the Galacto-light system (Applied Biosystems).

1. Grady RM, et al. (1997) Skeletal and cardiac myopathies in mice lacking utrophin and dystrophin: A model for Duchenne muscular dystrophy. *Cell* 90(4):729–738.
2. Yue Y, Liu M, Duan D (2006) C-terminal-truncated microdystrophin recruits dystrobrevin and syntrophin to the dystrophin-associated glycoprotein complex and reduces muscular dystrophy in symptomatic utrophin/dystrophin double-knockout mice. *Mol Ther* 14(1):79–87.
3. Lai Y, et al. (2009) Dystrophins carrying spectrin-like repeats 16 and 17 anchor nNOS to the sarcolemma and enhance exercise performance in a mouse model of muscular dystrophy. *J Clin Invest* 119(3):624–635.
4. Li D, Yue Y, Lai Y, Hakim CH, Duan D (2011) Nitrosative stress elicited by nNOSμ delocalization inhibits muscle force in dystrophin-null mice. *J Pathol* 223(1):88–98.

5. Rybakova IN, Patel JR, Davies KE, Yurchenco PD, Ervasti JM (2002) Utrophin binds laterally along actin filaments and can couple costameric actin with sarcolemma when overexpressed in dystrophin-deficient muscle. *Mol Biol Cell* 13(5):1512–1521.
6. Shin JH, Yue Y, Duan D (2012) Recombinant adeno-associated viral vector production and purification. *Methods Mol Biol* 798:267–284.
7. Zhong L, et al. (2008) Next generation of adeno-associated virus 2 vectors: Point mutations in tyrosines lead to high-efficiency transduction at lower doses. *Proc Natl Acad Sci USA* 105(22):7827–7832.
8. Qiao C, et al. (2010) AAV6 capsid tyrosine to phenylalanine mutations improve gene transfer to skeletal muscle. *Hum Gene Ther* 21(10):1343–1348.
9. Lai Y, et al. (2005) Efficient in vivo gene expression by trans-splicing adeno-associated viral vectors. *Nat Biotechnol* 23(11):1435–1439.
10. Morris G, Man NT, Sewry CA (2011) Monitoring duchenne muscular dystrophy gene therapy with epitope-specific monoclonal antibodies. *Methods Mol Biol* 709:39–61.
11. Li D, et al. (2010) Sarcolemmal nNOS anchoring reveals a qualitative difference between dystrophin and utrophin. *J Cell Sci* 123(Pt 12):2008–2013.
12. Li D, Shin JH, Duan D (2011) iNOS ablation does not improve specific force of the extensor digitorum longus muscle in dystrophin-deficient mdx4cv mice. *PLoS ONE* 6(6):e21618.
13. Li D, Long C, Yue Y, Duan D (2009) Sub-physiological sarcoglycan expression contributes to compensatory muscle protection in mdx mice. *Hum Mol Genet* 18(7):1209–1220.
14. Brenman JE, Chao DS, Xia H, Aldape K, Bredt DS (1995) Nitric oxide synthase complexed with dystrophin and absent from skeletal muscle sarcolemma in Duchenne muscular dystrophy. *Cell* 82(5):743–752.

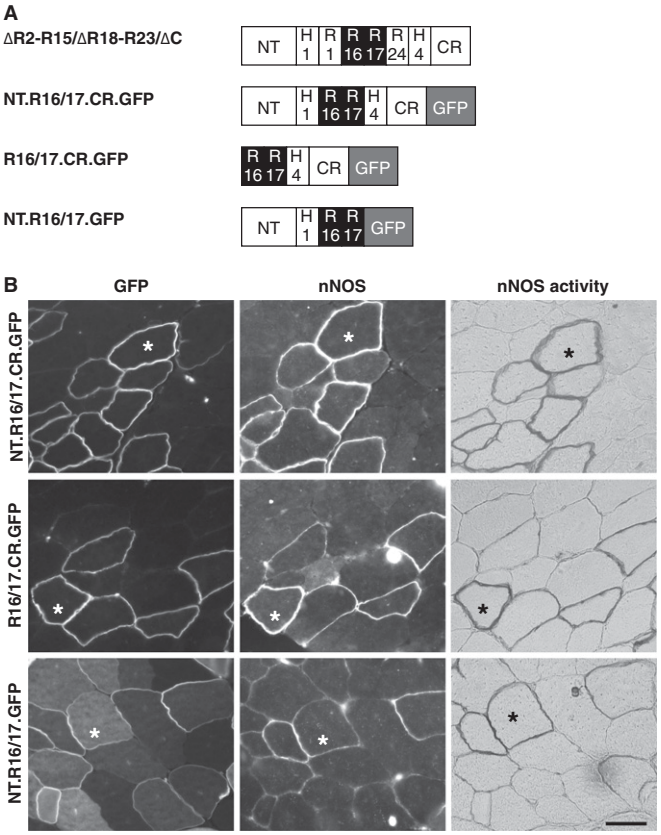

Fig. S1. Dystrophin spectrin-like repeats R16/17 independently recruit nNOS to the membrane. (*A*) Schematic outline of the microdystrophin constructs used in the study. The ΔR2-R15/ΔR18-R23/ΔC microgene can anchor nNOS to the sarcolemma. This microgene contains the N-terminal (NT) domain, an abbreviated rod domain consisting of hinges H1 and H4 and spectrin-like repeats R1, R16, R17, and R24, and the cysteine-rich (CR) domain. The remaining three microgenes all have a GFP tag fused at the C-terminal end. The NT.R16/17.CR.GFP microgene contains NT, H1, H4, R16, R17 and CR. The R16/17.CR.GFP microgene contains R16, R17, H4, and CR. The NT.R16/17.CR.GFP microgene contains NT, H1, R16, and R17. (*B*) Representative photomicrographs of GFP, nNOS immunostaining and nNOS activity staining from mdx mice infected with the indicated microdystrophin AAV virus. (*Top*) NT.R16/17.CR.GFP microgene AAV infected muscle; (*Middle*) R16/17.CR.GFP microgene AAV infected muscle; (*Bottom*) the NT.R16/17.GFP microgene AAV infected muscle. Asterisks indicate the same myofiber in the serial sections. (Scale bar, 50 μm.)

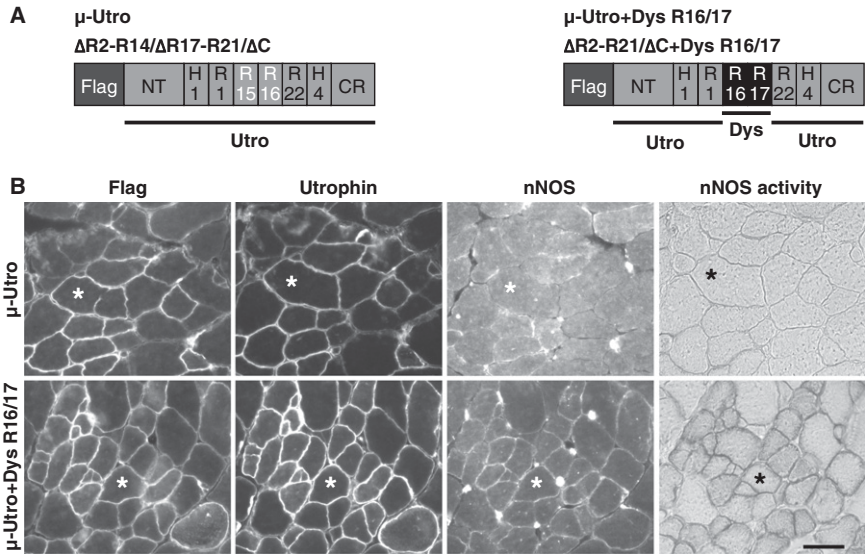

Fig. S2. Dystrophin R16/17 restores sarcolemmal nNOS expression in the context of microutrophin. (*A*) Schematic outline of the ΔR2-14/ΔR17-21/ΔC microutrophin gene (*Left*, μ-Utro) and the chimeric ΔR2-R21/ΔC+Dys R16/17 microutrophin gene (*Right*, μ-Utro+Dys R16/17). Utrophin R15/16 (highlighted in white) share homology with dystrophin R16/17. In the chimeric microutrophin gene, utrophin R15/16 was replaced by dystrophin R16/17. A flag tag was engineered at the N-terminal end of the microutrophin constructs to facilitate detection. (*B*) AAV viruses expressing the parental or the chimeric microutrophin genes were delivered to the anterior tibialis muscle of utrophin/dystrophin double knockout mice. Representative images of flag, utrophin, and nNOS immunofluorescence staining and nNOS activity staining. (*Upper*) ΔR2-14/ΔR17-21/ΔC microutrophin AAV infected; (*Lower*) ΔR2-R21/ΔC+Dys R16/17 chimeric microutrophin AAV infected. Asterisks indicate the same myofiber in the serial sections. (Scale bar, 50 μm.)

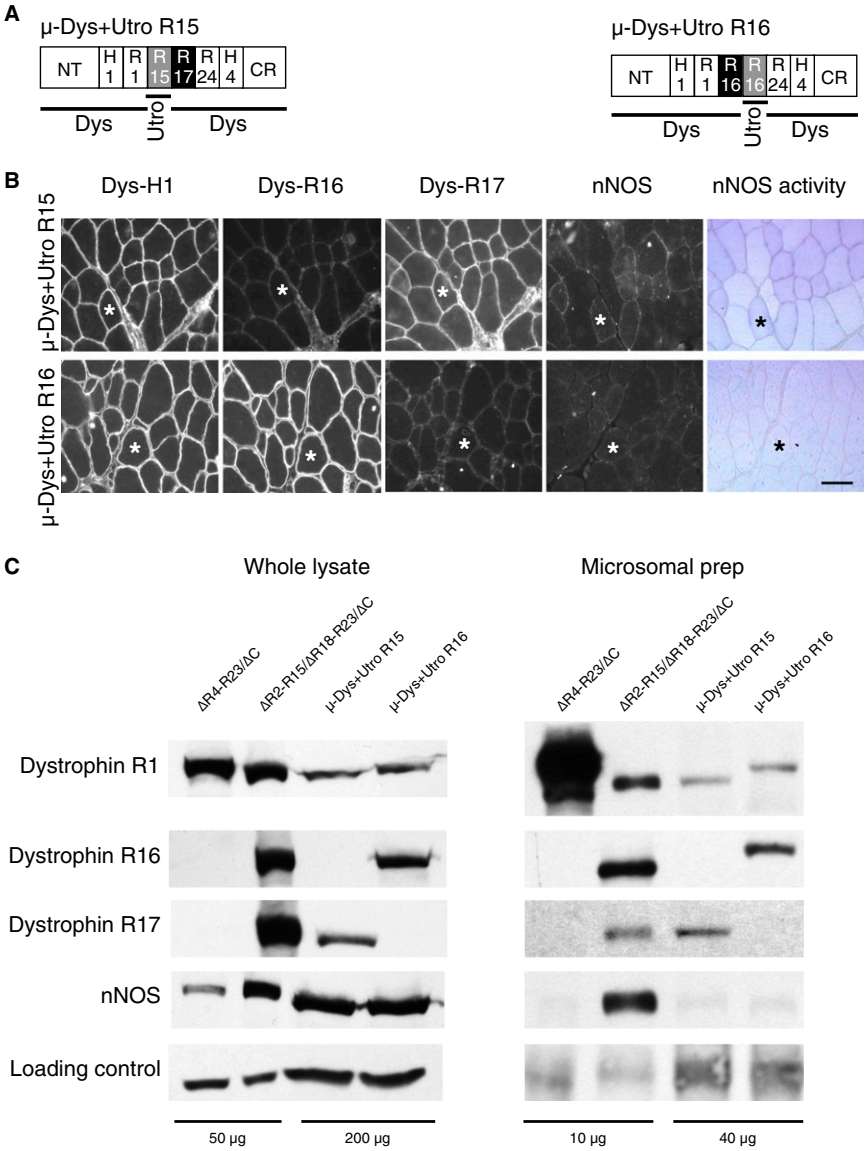

Fig. S3. Substitution of dystrophin R16 or 17 with respective utrophin R15 or R16 compromises nNOS membrane targeting by ΔR2-R15/ΔR18-R23/ΔC microdystrophin. (*A*) Schematic outline of the μ-Dys+Utro R15 and μ-Dys+Utro R16 chimerical microdystrophin constructs. In the μ-Dys+Utro R15 construct, dystrophin R16 is replaced by utrophin R15. In the μ-Dys+Utro R16 construct, dystrophin R17 is replaced by utrophin R16. (*B*) Representative images of dystrophin H1, R16, R17, and nNOS immunofluorescence staining and nNOS activity staining on the serial sections of chimerical microdystrophin AAV vector infected mdx muscle. Asterisks indicate the same myofiber in the serial sections. (Scale bar, 50 μm.) (*C*) Representative Western blot results from whole muscle lysate and microsomal preparation. ΔR4-R23/ΔC and ΔR2-R15/ΔR18-R23/ΔC are two transgenic mouse lines that specifically express microgenes in skeletal muscle. The ΔR4-23/ΔC microdystrophin gene does not contain dystrophin R16/17 (negative control). The ΔR2-R15/ΔR18-R23/ΔC microdystrophin gene contains dystrophin R16/17 (positive control). α-Tubulin was used as the loading control for whole muscle lysate. α1-Na^+/K^+ ATPase was used as the loading control for microsomal preparation.

Table S1. Summary of microdystrophin and microutrophin constructs used in the study

Construct name	Configuration	Lab log no.	Source
Microdystrophin			
ΔR2-R15/ΔR18-R23/ΔC	NT, H1, R1, R16, R17, R24, H4, CR	YL90	Fig. S1
NT.R16/17.CR.GFP	NT, H1, R16, R17, H4, CR, GFP	YL228	Fig. S1
R16/17.CR.GFP	R16, R17, H4, CR, GFP	YL230	Fig. S1
NT.R16/17.GFP	NT, H1, R16, R17, GFP	YL229	Fig. S1
R16/17.GFP	R16, R17, GFP	YL231	Fig. 1
R16/17.GFP.Pal	R16, R17, GFP, Pal	YL299	Fig. 1
Microutrophin and repeat-modified microutrophin			
μ-Utro (ΔR2-R14/ΔR17-R21/ΔC)	Flag, Utro(NT, H1, R1, R15, R16, R22, H4, CR)	YL239	Fig. S2
μ-Utro+Dys R16/17 (ΔR2-R21/ΔC+Dys R16/17)	Flag, Utro(NT, H1, R1), Dys R16, Dys R17, Utro(R22, H4, CR)	YL223	Fig. S2
Microdomain-modified microdystrophin			
Construct I	NT, H1, R1, R16(Utro microdomain VYKDFSF), R17, R24, H4, CR	YL278	Fig. 2
Construct II	NT, H1, R1, R16(Utro microdomain DRLGEQ), R17, R24, H4, CR	YL279	Fig. 2
Construct III	NT, H1, R1, R16(Utro microdomain IAVVHEK), R17, R24, H4, CR	YL280	Fig. 2
Construct IV	NT, H1, R1, R16(Utro microdomain QPDVIVE), R17, R24, H4, CR	YL281	Fig. 2
Construct V	NT, H1, R1, R16(Utro microdomain SGPEAIQIRD), R17, R24, H4, CR	YL282	Fig. 2
Construct VI	NT, H1, R1, R16(Utro microdomain MLAQLNAKW), R17, R24, H4, CR	YL283	Fig. 2
Construct VII	NT, H1, R1, R16(Utro microdomain DRVNRVYS), R17, R24, H4, CR	YL284	Fig. 2
Construct VIII	NT, H1, R1, R16(Utro microdomain DRRGS), R17, R24, H4, CR	YL285	Fig. 2
Construct IX	NT, H1, R1, R16, R17(Utro microdomain QFHHDLDDLT), R24, H4, CR	YL286	Fig. 2
Construct X	NT, H1, R1, R16, R17(Utro microdomain DLLVDTC), R24, H4, CR	YL287	Fig. 2
Construct XI	NT, H1, R1, R16, R17(Utro microdomain DGSLDLEKARA), R24, H4, CR	YL288	Fig. 2
Construct XII	NT, H1, R1, R16, R17(Utro microdomain QQLELEE), R24, H4, CR	YL289	Fig. 2
Construct XIII	NT, H1, R1, R16, R17(Utro microdomain SSHQPSLI), R24, H4, CR	YL290	Fig. 2
Construct XIV	NT, H1, R1, R16, R17(Utro microdomain KVNRKGED), R24, H4, CR	YL291	Fig. 2
Microdomain-modified microutrophin			
μ-Utro+Dys R17 microdomain IX	Flag, Utro (NT, H1, R1, R15, R16(Dys R17 microdomain IX), R22, H4, CR)	YL325	Fig. 3
Linker region-modified microdystrophin			
Mutant-1	NT, H1, R1, R16(Utro R15 3′-linker sequence), R17, R24, H4, CR	YL312	Table S2
Mutant-2	NT, H1, R1, R16(Dys R15 3′-linker sequence), R17, R24, H4, CR	YL313	Table S2
Mutant-3	NT, H1, R1, R16(Dys repeat 3′- linker consensus sequence), R17, R24, H4, CR	YL314	Table S2
Mutant-4	NT, H1, R1, R16, R17(Utro R16 5′-linker sequence), R24, H4, CR	YL315	Table S2
Repeat-modified microdystrophin			
μ-Dys+Utro R15	NT, H1, R1, Utro(R15), R17, R24, H4, CR	YL310	Fig. S3
μ-Dys+Utro R16	NT, H1, R1, R16, Utro(R16), R24, H4, CR	YL311	Fig. S3
Helix-deleted microdystrophin			
ΔR16-α1	NT, H1, R1, R16(α2, α3), R17, R24, H4, CR	YL180	Fig. 5*A*
ΔR16-α2	NT, H1, R1, R16(α1, α3), R17, R24, H4, CR	YL181	Fig. 5*A*
ΔR16-α3	NT, H1, R1, R16(α1, α2), R17, R24, H4, CR	YL182	Fig. 5*A*
ΔR17-α1	NT, H1, R1, R16, R17(α2, α3), R24, H4, CR	YL183	Fig. 5*A*
ΔR17-α2	NT, H1, R1, R16, R17(α1, α3), R24, H4, CR	YL184	Fig. 5*A*
Helix-substituted microdystrophin			
R16 α1#	NT, H1, R1, R18(α1)+R16(α2, α3), R17, R24, H4, CR	YL232	Fig. 5*B*
R16 α2#	NT, H1, R1, R16(α1)+R18(α2)+R16(α3), R17, R24, H4, CR	YL233	Fig. 5*B*
R16 α3#	NT, H1, R1, R16(α1, α2)+R18(α3), R17, R24, H4, CR	YL234	Fig. 5*B*
R17 α2#	NT, H1, R1, R16, R17(α1)+R18(α2)+R17(α3), R24, H4, CR	YL236	Fig. 5*B*
R17 α3#	NT, H1, R1, R16, R17(α1, α2)+R18(α3), R24, H4, CR	YL273	Fig. 5*B*
R16 α1#+R17#	NT, H1, R1, R2(α1)+R16(α2, α3), R3, H2, R24, H4, CR	YL270	Table S2
R16#+R17α3#	NT, H1, R1, R2, R17(α1, α2)+R3(α3), H2, R24, H4, CR	YL271	Table S2
R16 α1#+R17 α3#	NT, H1, R1, R2(α1)+R16(α2, α3), R17(α1, α2)+R3(α3), H2, R24, H4, CR	YL272	Table S2
R17 α1#	NT, H1, R1, R16, R18(α1)+R17(α2, α3), R24, H4, CR	YL235	Table S2
R16 α2 with R4 α2	NT, H1, R1, R16(α1)+R4(α2)+R16(α3), R17, R24, H4, CR	YL382	Table S2
R16 α3 with R4 α3	NT, H1, R1, R16(α1, α2)+R4(α3), R17, R24, H4, CR	YL383	Table S2
R17 α2 with R5 α2	NT, H1, R1, R16, R17(α1)+R5(α2)+R17(α3), R24, H4, CR	YL384	Table S2
R17 α3 with R5 α3	NT, H1, R1, R16, R17(α1, α2)+R5(α3), R24, H4, CR	YL385	Table S2

Constructs are listed in the order as they appear in the manuscript. CR, cystein-rich domain; H, hinge; NT, N-terminal domain; Pal, palmitoylation membrane targeting sequence; R, spectrin-like repeat; Utro, utrophin.

Table S2. Impact of indicated mutation on nNOS binding in vivo

Construct name	Configuration*	Lab log no.	nNOS binding
Linker region-modified microdystrophin			
Original linker sequence (R16/R17)	FDR/SVEK		
Mutant-1	F**A**R/SVEK	YL312	Yes
Mutant-2	F**AQ**/SVEK	YL313	Yes
Mutant-3	**LEE**/SVEK	YL314	Yes
Mutant-4	FDR/**AVEE**	YL315	Yes
Helix-substituted microdystrophin			
Original configuration (R16/R17)	R16(α1),R16(α2),R16(α3)/R17(α1),R17(α2),R17(α3)		
R16 α1#+R17#	**R2(α1)**,R16(α2),R16(α3)/**R3(α1),R3(α2),R3(α3)**	YL270	No
R16#+R17α3#	**R2(α1),R2(α2),R2(α3)**/R17(α1),R17(α2),**R3(α3)**	YL271	No
R16 α1#+R17 α3#	**R2(α1)**,R16(α2),R16(α3)/R17(α1),R17(α2),**R3(α3)**	YL272	No
R17 α1#	R16(α1),R16(α2),R16(α3)/**R18(α1)**,R17(α2),R17(α3)	YL235	No
R16 α2 with R4 α2	R16(α1),**R4(α2)**,R16(α3)/R17(α1),R17(α2),R17(α3)	YL382	No
R16 α3 with R4 α3	R16(α1),R16(α2),**R4(α3)**/R17(α1),R17(α2),R17(α3)	YL383	No
R17 α2 with R5 α2	R16(α1),R16(α2),R16(α3)/R17(α1),**R5(α2)**,R17(α3)	YL384	No
R17 α3 with R5 α3	R16(α1),R16(α2),R16(α3)/R17(α1),R17(α2),**R5(α3)**	YL385	No

*Mutation is highlighted in boldface letters.